

Bacterial Hydrodynamics*

Eric Lauga[†]

Department of Applied Mathematics and Theoretical Physics, Centre for Mathematical Sciences, University of Cambridge, Wilberforce Road, Cambridge, CB3 0WA, United Kingdom

(Dated: March 5, 2022)

Bacteria predate plants and animals by billions of years. Today, they are the world's smallest cells yet they represent the bulk of the world's biomass, and the main reservoir of nutrients for higher organisms. Most bacteria can move on their own, and the majority of motile bacteria are able to swim in viscous fluids using slender helical appendages called flagella. Low-Reynolds-number hydrodynamics is at the heart of the ability of flagella to generate propulsion at the micron scale. In fact, fluid dynamic forces impact many aspects of bacteriology, ranging from the ability of cells to reorient and search their surroundings to their interactions within mechanically and chemically-complex environments. Using hydrodynamics as an organizing framework, we review the biomechanics of bacterial motility and look ahead to future challenges.

I. INTRODUCTION

Bacteria constitute the bulk of the biomass of our planet. However, since we need a microscope to see them, we often forget their presence. Observing life in the ocean, we see fish and crustaceans, but miss the marine bacteria that outnumber them many times over. On land, we see animals and plants, but often forget that a human body contains many more bacteria than mammalian cells. While they are responsible for many infectious diseases, bacteria play a critical role in the life of soils and higher organisms (including humans) by performing chemical reactions and providing nutrients (Madigan et al., 2010).

Ever since microscopes were invented, scientists have worked to decipher the rules dictating the behavior of bacteria. In addition to quantifying the manner in which bacteria shape our lives and teach us about our evolutionary history, biologists have long recognized that the behavior of bacteria is influenced by the physical constraints of their habitat, and by their evolution to maximize fitness under these constraints. The most prominent of these constraints is the presence of a surrounding fluid (Vogel, 1996). Not only are all bacteria found in fluids, but being typically less than a hundredth of a millimeter in length, they experience much larger viscous forces than inertial forces, and have adapted their behavior in response to these forces.

Most bacteria are motile (Jarrell & McBride, 2008; Kearns, 2010) and this motility is essential for the effectiveness of many pathogens (Ottemann & Miller, 1997). The most common form of bacterial motility is swimming. In order to swim, bacteria have evolved flagella (originally from secretory systems), which are slender helical appendages rotated by specialized motors, and whose motions in viscous environments propel the

cells forward (Bray, 2000). The surrounding fluid can be seen both as a constraint and an advantage. It is the presence of the fluid itself and its interactions with three-dimensional bacterial flagellar filaments which allows cells to move and sample their chemical environment – a crucial step for the cells to display robust and adaptive chemotactic responses to both attractants and repellents, for nutrients, but also temperature, pH, and viscosity (Berg, 1993, 2004; Blair, 1995; Purcell, 1977).

But as they self-propel, bacteria are subject to the external constraints set by the physical world, and in particular by hydrodynamics. In this review, we highlight the consequences of fluid dynamics relevant to the swimming of bacteria in viscous environments. Naturally, the biophysics of bacteria locomotion involves many aspects of soft matter physics, including nonlinear elasticity, screened electrostatics, and biochemical noise, and hence fluid dynamics represents but one feature of the complex balance of forces dictating the behavior of cells as they search their environment. The choice made here is to use hydrodynamics as an organizing framework to overview various aspects of cellular locomotion.

We start by a biological overview of bacteria as cells, their geometry, the way they swim, and the variations among different species (§II). We then review the basic hydrodynamics features of flagellar propulsion (§III) followed by the flows induced by swimming bacteria (§IV). We next address the flagellar polymorphs, their comparative hydrodynamics, and the potential relevance to evolution of the flagellum (§V). With individual flagella understood, we detail how fluid forces may play a role in the actuation of multiple flagella and be used by cells to reorient (§VI). The last three sections are devoted to locomotion near surfaces (§VII), in external flows (§VIII) and in complex fluids (§IX).

Throughout this review, the focus will be on single-cell behavior. Our purpose is to understand the way a single bacterium exploits, and is subject to, the physical constraints from the surrounding fluid. Other useful reviews can be used as complementary reading, in particular those highlighting the hydrodynamics of low-

*to appear in: Annu. Rev. Fluid Mech. **48** (2016)

[†]e.lauga@damtp.cam.ac.uk

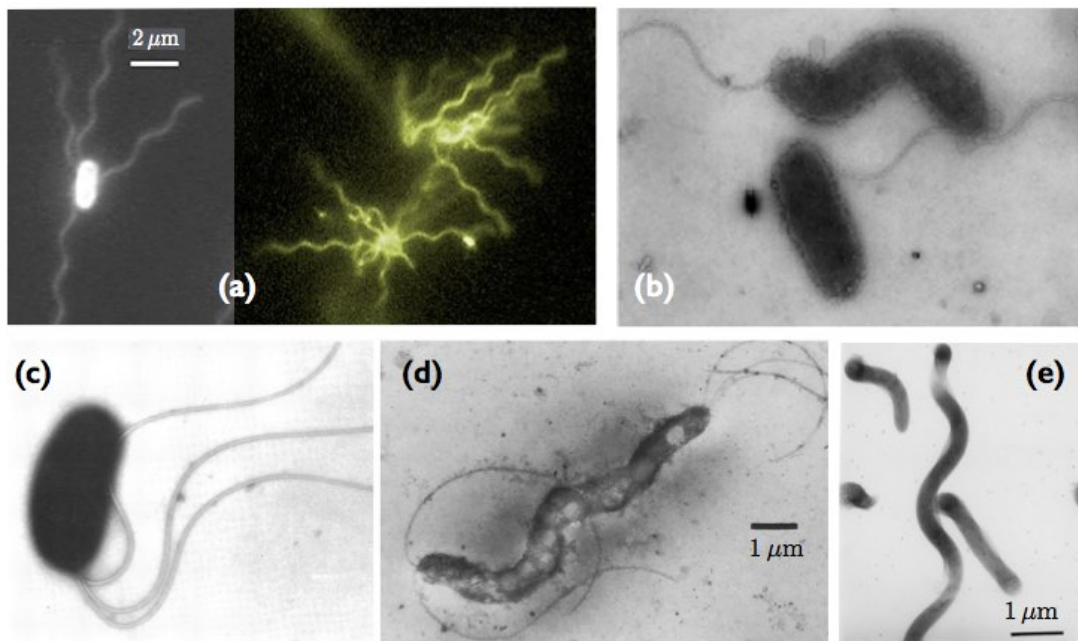


FIG. 1 Atlas of flagellated bacteria. (a) Peritrichous *Escherichia coli* (Howard Berg, Harvard University); (b) Polar monotrichous *Pseudomonas aeruginosa* (Fujii et al., 2008); (c) Polar lophotrichous *Photobacterium fischeri* (Allen & Baumann, 1971); (d) Polar amphitrichous *Ectothiorhodospira hatochtoris* (Imhoff & Trüper, 1977); (e) Spirochetes with endoflagella *Borrelia burgdorferi* (Goldstein et al., 1996). All figures reproduced with permission.

Reynolds number swimming (Brennen & Winet, 1977; Lauga & Powers, 2009; Lighthill, 1975), the fluid dynamics of plankton (Goldstein, 2015; Guasto et al., 2012; Pedley & Kessler, 1992), reproduction (Fauci & Dillon, 2006; Gaffney et al., 2011), and collective cell locomotion (Koch & Subramanian, 2011).

II. BIOLOGICAL ATLAS

Bacteria come in many different shapes (Madigan et al., 2010). Those able to swim in fluids can be roughly divided into two categories: bacteria whose propulsion is driven by helical flagellar filaments located outside a non-deforming cell body (the overwhelming majority, illustrated in Fig. 1a-d) and those with spiral-like body undergoing time-varying deformation (Fig. 1e).

Our understanding of how flagellated bacteria swim has its roots in a series of investigations in the 1970s showing conclusively that – unlike the active flagella of eukaryotes, which are active and muscle-like (Bray, 2000) – bacterial flagellar filaments are passive organelles (Berg & Anderson, 1973; Silverman & Simon, 1974). Typically a few to ten microns in length, and only 40 nm in diameter, bacterial flagellar filaments are helical polymers whose structure is discussed in detail in §V. Each filament is attached to a short flexible hook (≈ 60 nm in length, see Fig. 2) acting as a universal joint. The hook is turned by a stepper motor driven by ion fluxes (bacterial rotary motor, Fig. 2) which is well characterized

molecularly (Berg, 2003).

Some flagellated cells are called *peritrichous* and have many motors (and thus many flagella) located randomly at various positions on the cell body (Fig. 1a). This is the case for the bacterium *Escherichia coli* (or *E. coli*), chosen as a model organism to study the fundamental biophysical aspects of cell motility and chemotaxis (Berg, 2004). In contrast, *polar* bacteria have motors only located at poles of the body. Of the polar bacteria, *monotrichous* bacteria only have one motor, and thus one filament (Fig. 1b), *lophotrichous* cells have a tuft of flagella originating from a single pole (Fig. 1c) while *amphitrichous* bacteria have flagella at each pole (Fig. 1d). Note that variations in this classification exist; for example, some monotrichous or lophotrichous bacteria are not polar. In all cases, the rotation of the motor is transmitted to the hook, which in turn transmits it to the helical filament, leading to the generation of hydrodynamic propulsive forces, as explained in detail in §III.

Fluid dynamics was used to determine the torque-frequency relationship for the rotary motor by linking tethered bacterial flagella to beads of different sizes in fluids of varying viscosity (Chen & Berg, 2000). The resulting change in the Stokes resistance to bead rotation allowed to show that the rotary motor works at constant torque for a wide range of frequencies in the counter-clockwise (CCW) directions (the frequency range depends strongly on temperature) before showing a linear decrease of the torque at higher frequencies (Berg, 2003). In contrast, when rotating in the clockwise (CW) direc-

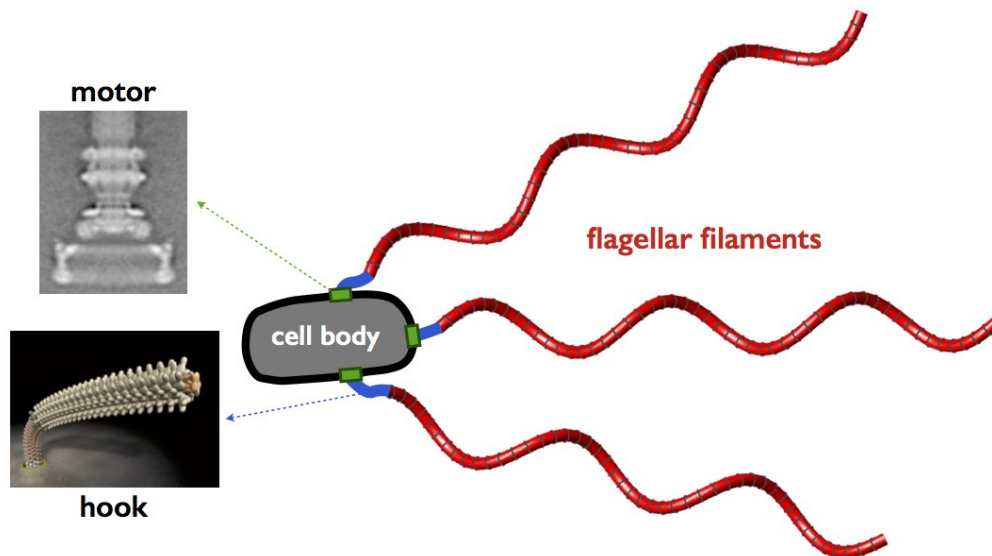


FIG. 2 Schematic representation of a peritrichous bacterium with three flagellar filaments showing a bacterial rotary motor embedded in the cell wall (the stator part of the motor is not shown) (Berg, 2003) and a hook with its junction to a flagellar filament (K. Namba, Osaka University). All figures reproduced with permission.

tion, the motor torque linearly decreases with frequency (Yuan et al., 2010).

In the range relevant to locomotion, the motor can be assumed to behave as continuously rotating and producing a constant torque. The value of this torque is however still under debate and measurements are at odds with theoretical predictions. While its stall torque has been experimentally estimated to be on the order of 4,600 pN nm (Berry & Berg, 1997), experiments using beads lead to the conclusion that the motor has to be on the range 1260 ± 190 pN nm (Reid et al., 2006). In contrast, theoretical estimates using a simplified model for the fluid predict a significantly smaller value of 370 ± 100 pN nm (Darnton et al., 2007).

While the majority of swimming bacteria are powered by flagellar filaments rotating in the fluid outside the cells, two other modes of locomotion in fluids are notable. Bacteria of the spirochete family have a spiral shape and undergo whole-body undulations powered also by flagella (Fig. 1e). However, in this case, the filaments are constrained in the small space between the cytoplasmic membrane and outer membrane of the cell body, and it is the rotation in this tight space which leads to wave-like whole-body undulations and in turn leads to locomotion in a fluid (Vig & Wolgemuth, 2012). Swimming without flagella has also been reported for *Spiroplasma*, a type of helical bacterium whose body has no cell wall. In that case, a wavelike motion is induced by contraction of the cell cytoskeleton leading to the propagation of shape kinks along the body (Shaevitz et al., 2005; Wada & Netz, 2007). At least one other bacterium, the marine *Synechococcus*, swims in fluids in manner which is as yet undetermined (Ehlers & Oster, 2012).

To close this biological overview, we mention the other mode of fluid-based motility termed swarming (Jarrell & McBride, 2008; Kearns, 2010). A few bacterial families, when present in media-rich in nutrients, can undergo a differentiation to a swarming state, where they become more elongated, grow more flagella and swim in closely-packed groups, the physics of which is only beginning to be unraveled (Copeland & Weibel, 2009; Darnton et al., 2010).

III. HYDRODYNAMICS OF HELICAL PROPULSION

The most fundamental aspect of bacterial hydrodynamics is the ability of rotating flagella to produce propulsive forces (Chwang & Wu, 1971; Higdon, 1979; Lighthill, 1976). At the origin of this generation of forces is the non-isotropic nature of hydrodynamic friction in the Stokesian regime (Brennen & Winet, 1977; Lauga & Powers, 2009). At the low Reynolds numbers relevant to swimming bacteria (typically ranging from 10^{-4} to 10^{-2}), the flows are governed by the incompressible Stokes equations, and drag forces on rigid bodies scale linearly with their instantaneous velocities relative to the background fluid. Because flagellar filaments are slender (their aspect ratio is at least 100), their physics can be intuitively understood by analogy with the motion of a rod. At a given velocity, a rod experiences a drag from the fluid about twice as large when translating perpendicular to its long axis as that when moving along it. For a non-symmetric velocity/rod orientation, the hydrodynamic drag on the rod is thus not aligned with the direction of its velocity but possesses a nonzero component perpendicular to it – hence the possibility of drag-based

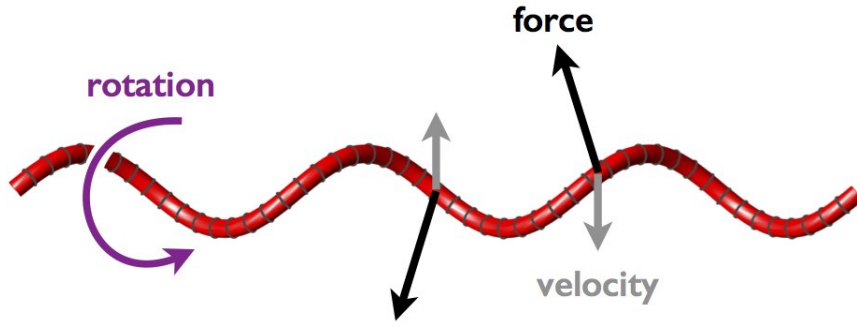


FIG. 3 Hydrodynamics of propulsion by a rotating helical flagellar filament. A left-handed helix rotates in the CCW direction (when viewed from the right) as indicated by a purple arrow. The local velocity of two material points on the helix relative to the background fluid are illustrated with gray arrows. Since the fluid drag is larger (for a given velocity) for motion of the local helix perpendicular than parallel to the local tangent, the net force density from the fluid includes a component directed everywhere along the helix axis (black arrows). A net moment opposing the rotation is also generated, resulting in counter-rotation of the cell.

thrust.

The extension of this idea to case of a helical filament is illustrated in Fig. 3. The flagellar filament is taken here to be left-handed and undergoes CCW rotation when viewed from the right looking left (more on this in §V). The local velocity of two material points on the helix is illustrated by gray arrows: points in the foreground go down while points in the background go up. The instantaneous drag force density resisting the rotation of the helix in the fluid is illustrated by black arrows. Because of the higher resistance from the projection of the local velocity in the direction perpendicular to the local tangent to the helix, the total drag includes a nonzero component along the axis of the helix, which in both cases points to the left along the helix axis (this is exaggerated in the figure for illustration purposes). Consequently, a rotating helix is subject to a net viscous force aligned with the helix axis with an orientation which depends on the handedness of the helix and the direction of rotation.

From a Stokes flow standpoint, the grand resistance matrix for a helical flagellar filament, which linearly relates forces and moments to velocities and rotation rates, includes therefore an off-diagonal term coupling axial rotation with axial force (Kim & Karrila, 1991; Purcell, 1997). Because the whole cell is force-free, it has to swim in order to balance this force. This is the physical mechanism used by bacteria to self-propel in fluids, and it will in fact be intuitive to anybody having opened a bottle of wine with a corkscrew where the rotation of the screw induces its translation inside the cork. As a difference with a corkscrew however, the propulsion of a helix in a viscous fluid produced by its rotation is very inefficient, both kinematically (small forward motion per rotation) and energetically (only a few percent of the total work done by the helix is transmitted to propulsive work) (Chattopadhyay et al., 2006; Purcell, 1997; Spagnolie & Lauga, 2011). The same hydrodynamic principles can be exploited to design artificial helical swimmers

powered by rotating magnetic fields (Ghosh & Fischer, 2009; Zhang et al., 2010). A famous illustration of helical locomotion in fluids is provided in G.I. Taylor’s movie on low Reynolds number flows (Taylor, 1967).

In addition to forces, the rotating filament in Fig. 3 is subject to a net hydrodynamic moment resisting the rotation. In order for the bacterium to remain torque-free, the cell body needs therefore to counter-rotate. With flagella typically rotating at ≈ 100 Hz, this is achieved by a counter-rotation at smaller frequency ≈ 10 Hz due to small rotational mobility of a large cell body (Chwang & Wu, 1971; Magariyama et al., 1995). Because of this balance of moments, locomotion powered by helical flagella is not possible in the absence of a cell body, a result qualitatively different from locomotion induced by planar waving deformation, for which a head is not required (Lauga & Powers, 2009). The resulting motion of a bacterium in a fluid consists thus of flagellar filaments rotating, the cell body counter-rotating, and the whole cell moving forward approximately in a straight line, or in helices of small amplitude when the axis of the filaments is not aligned with that of the cell body (Hyon et al., 2012; Keller & Rubinow, 1976). In general the cell body does not induce additional propulsion, which is all due to the flagella, unless it is the right shape and has the right orientation relative to the helical flagellum (Chwang et al., 1972; Liu et al., 2014b).

The hydrodynamic theories developed to calculate the distribution of forces on rotating helical flagella are of three flavors (Brennen & Winet, 1977; Lauga & Powers, 2009). The first one, historically, considered the theoretical limit of very (exponentially) slender filaments to compute forces as a perturbation expansion in the logarithm of the aspect ratio of the flagella. At leading order, this so-called resistive-force theory predicts that the local force density at one point along the filament is proportional to its local velocity relative to the fluid with a coefficient of proportionality which depends on the relative

orientation of the velocity with respect to the local tangent (Cox, 1970; Gray & Hancock, 1955; Lighthill, 1975). This is therefore the natural extension of the physical picture discussed above for rigid rods to deforming filaments. While this is the most widely used approach, and one which is able to provide basic physical pictures, it is often not sufficiently accurate as the associated relative errors are only logarithmically small (Chattopadhyay & Wu, 2009; Johnson & Brokaw, 1979). More precise is the second approach, termed slender-body theory, which consists in distributing appropriate flow singularities of suitable strengths in order to match the boundary condition on the surface of the filament at a required, algebraically small, precision (Hancock, 1953; Johnson, 1980; Lighthill, 1976). In that case the equation relating the distribution of velocity to the distribution of forces is non-local, because of long-range hydrodynamic interactions, and thus needs to be inverted numerically. A final option is to use fully three-dimensional computations. The most common method is an integration of the equations of Stokes flows using either boundary elements (Liu et al., 2013; Phan-Thien et al., 1987), regularized flow singularities (Flores et al., 2005; Olson et al., 2013), or immersed boundaries (Fauci & Dillon, 2006). Mesoscopic particle-based methods have recently been proposed as an alternative approach (Reigh et al., 2012).

IV. FLOWS INDUCED BY BACTERIA

The general fluid dynamics picture of a swimming bacterium powered by the rotation of a flagellum is illustrated in Fig. 4a. We use purple arrows to indicate the local forcing of the swimming cell on the surrounding fluid. Near the filament, the induced flow is a combination of rotation and polar axial pumping directed away from the cell body. This is illustrated in Fig. 4b-c using slender-body theory for a helical waveform of diameter 400 nm and wavelength $2.3 \mu\text{m}$ (the so-called “normal” waveform, see discussion in §V) (Spagnolie & Lauga, 2011).

Looking further away from the cell, because the swimming bacterium is force-free, it pushes on the fluid with an equal and opposite force to the one generated by the rotating filament (Fig. 4a), and thus the leading order flow in the far-field is a force-dipole, or stresslet, as schematically illustrated in Fig. 4c (Batchelor, 1970; Ishikawa et al., 2007). The type of associated dipole is termed a pusher, in contrast with puller dipoles relevant to cells which swim flagella first, for example planktonic bi-flagellates (Guasto et al., 2012). This flow has been measured for swimming *E. coli* using an experimental tour-de-force (Drescher et al., 2011). The magnitude of the induced flow is shown in Fig. 4e (in $\mu\text{m/s}$), while the theoretical dipolar prediction is shown in Fig. 4f, with a difference shown in Fig. 4g. The dipole strength is on the order of $0.1 - 1 \text{ N } \mu\text{m}$ (Berke et al., 2008; Drescher et al., 2011) and this dipolar picture is very accurate up to a few body lengths away, at which point the flow speeds

get overwhelmed by thermal noise.

While the leading-order flow is a stresslet decaying spatially as $1/r^2$, the velocity field around a bacterium also includes higher-order (decaying as $1/r^3$) flow singularities which are important in the near field. These include source-dipoles and force quadrupoles (Chwang & Wu, 1975). Force-quadrupoles, for example, dominate velocity correlations between swimming bacteria, because force-dipoles are front-back symmetric (Liao et al., 2007). An important flow near a swimming bacterium is a rotlet-dipole. Since the flagellum and the cell body rotate relative to the fluid in opposite directions (Fig. 4a), they act on the fluid as two point moments (or rotlets) of equal and opposite strengths, hence a rotlet-dipole, decaying spatially as $1/r^3$, and shown schematically in Fig. 4h (a rotlet dipole is a particular force quadrupole). A computational illustration of the streamlines associated with this flow is shown in Fig. 4i (Watari & Larson, 2010). Note that both the force-dipole and the rotlet-dipole can be time-dependent, and in some cases induce instantaneous flows stronger than their time averages (Watari & Larson, 2010).

The flows induced by swimming cells have been useful in understanding two problems. First, flows created by populations of bacteria lead to enhanced transport in the fluid. In addition to Brownian motion, passive tracers (for example nutrient molecules, or much larger suspended particles) also feel the sum of all hydrodynamic flows from the population of swimming bacteria, and in general will thus display an increase in the rate at which they are transported. Enhanced diffusion by swimming bacteria was first reported experimentally for flagellated *E. coli* cells with non-Brownian particles (Wu & Libchaber, 2000), followed by work on molecular dyes (Kim & Breuer, 2004). Dilute theories and simulations based on binary collisions between swimmers (possibly with a finite persistence time or finite run length) and passive tracers (possibly Brownian) have allowed to predict diffusion constants (Kasyap et al., 2014; Lin et al., 2011; Miño et al., 2013; Pushkin et al., 2013). In particular, it was shown that the extra diffusivity remains linear with the concentration of bacteria well beyond the dilute regime. The effect, while negligible for small molecules with high Brownian diffusivity, can be significant for large molecules or non-Brownian tracers.

The second topic where swimming-induced flows are critical is that of collective swimming. Suspension of swimming bacteria display modes of locomotion qualitatively different from individual cells, with long orientation and velocity correlation lengths, instabilities, and an intrinsic randomness – a process recently referred to as *bacterial turbulence*. Building on the standard theoretical description for Brownian suspensions (Doi & Edwards, 1988), the modeling approach consists in describing the populations of swimming bacteria as continua using a probability density function in orientation and position. Conservation of probability then establishes a balance between changes in bacteria configurations and

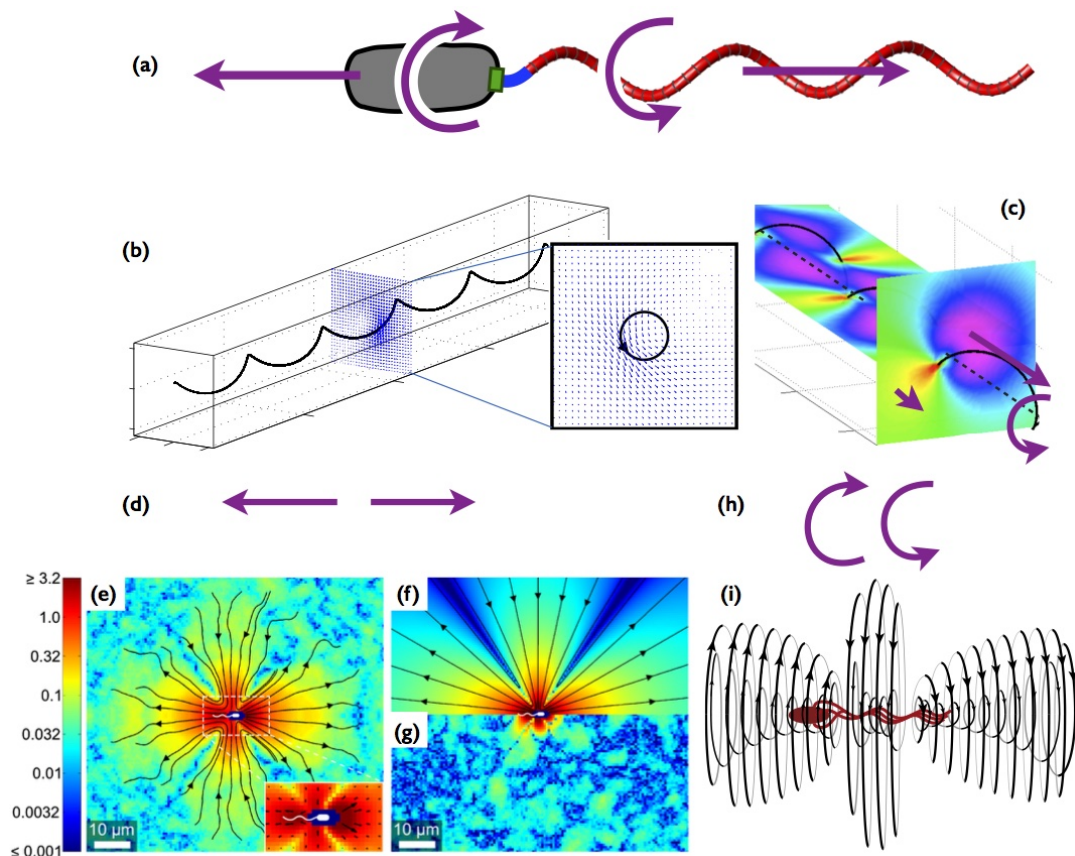


FIG. 4 The flows produced by swimming bacteria. (a) Schematic representation of the forcing induced locally by the bacterium on the surrounding fluid (purple arrows); (b) Rotational flow near a rotating helical filament (Spagnolie & Lauga, 2011); (c) Axial flow along the axis of the helical filament, directed away from the cell body; (d) In the far-field, the cell acts on the fluid as a force dipole; (e) Measurement of the flow induced by swimming *E. coli* (Drescher et al., 2011); (f) Theoretical prediction from force dipole; (g) Difference between measurement and theoretical prediction; (h) The rotation of the helical filament and the counter rotation of the cell body acts on the fluid as a rotlet dipole; (i) Simulation of this rotational flow with streamlines (Watari & Larson, 2010). All figures reproduced with permission.

diffusion, with changes in both position and orientation which are brought about by the flows (and their gradients) induced by the swimming bacteria. While the current article is focused on single-cell behaviour, we refer to the recent Annual Review on the topic (Koch & Subramanian, 2011) and book (Spagnolie, 2015), and references therein, for a more detailed overview.

V. POLYMORPHISM AND THE EVOLUTIONARY ROLE OF HYDRODYNAMICS

It is one of nature's wonders that bacterial flagellar filaments only exist in discrete helical shapes called flagellar polymorphs (Calladine, 1978; Hasegawa et al., 1998; Namba & Vonderviszt, 1997). Each filament is a polymer composed of a single protein (flagellin) which assembles in long protofilaments. Eleven of these protofilaments wrap around the circumference of the filament. Because flagellin (and thus each protofilament) exists in two dis-

tinct conformation states, an integer number of different conformations is available for the flagellum, of which only twelve are molecularly and mechanically stable (Calladine, 1978; Srigiriraju & Powers, 2006). These are the helical "polymorphic" shapes, illustrated in Fig. 5a. Of these 12 shapes, 2 are straight, and 10 are true helices. Of these 10 helices, 9 have been observed experimentally, induced by chemical, mechanical or temperature modifications (Hotani, 1980, 1982; Leifson, 1960). Of the 10 non-straight shapes, 3 are left-handed – including the most common one, called "normal," whose polymorphic number is #2 – and 7 are right handed – including the important "semi-coiled," which is #4, and "curly," which is #5.

As an elastic body, the force-extension curve of individual flagellar filaments and the transitions between the different polymorphs have been precisely characterized experimentally using optical tweezers pulling on filaments attached to a glass surface (Darnton & Berg, 2007). Fitting the data to a Kirchhoff elastic rod model with multiple

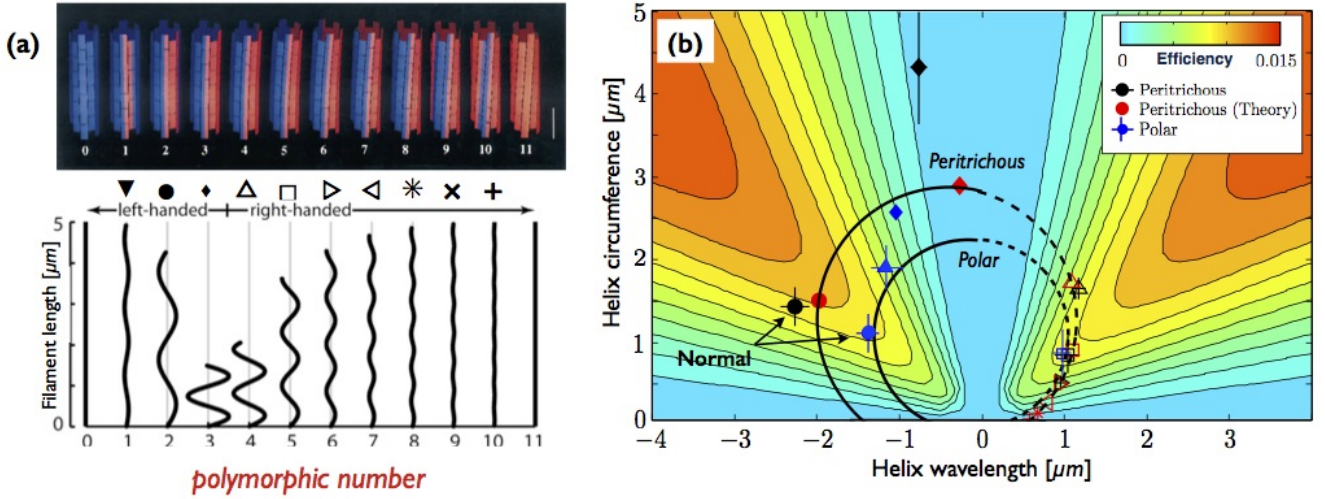


FIG. 5 (a) Illustration of the twelve polymorphic shapes of bacterial flagella, numbered #0 to #11 (Darnton et al., 2007; Hasegawa et al., 1998); (b) The intrinsic hydrodynamic efficiencies of each polymorph for Calladine’s theory (red) and for experimentally-measured peritrichous (black) and polar (blue) flagellar polymorphs (Purcell, 1997; Spagnolie & Lauga, 2011). Left (resp. right)-handed helices are denoted with negative (resp. positive) wavelengths and the corresponding waveform with filled (resp. empty) symbols, as seen in Fig. 5a. The circles allow differentiating peritrichous from polar polymorphs. All figures reproduced with permission.

minima for curvature and twist allows then to determine the elastic constants around polymorphic minima. The bending rigidities so estimated are on the order of few $\text{pN } \mu\text{m}^2$, and the transition forces from one shape to the next are on the order of a few pN (Darnton & Berg, 2007). A variety of associated modeling approaches for flagellar mechanics have been developed to reproduce these experimental results (Vogel & Stark, 2010; Wada & Netz, 2008). That flagellar filaments are elastic means they might deform under rotation, but during normal swimming conditions this has been shown to be a small effect (Kim & Powers, 2005). It is however possible that the moments and forces from the fluid induce buckling of a rotating filament, similar to elastic rods buckling under their own weight. While the threshold rotation rates appear to be close to biological numbers (Vogel & Stark, 2012), no sign of flagellar buckling has been reported so far.

The fact that different shapes exist is important for locomotion because, as we see in the next section, when a bacterium turns, the direction of rotation of one (or more) bacterial motor is changing, which induces a rapid polymorphic transformation for the associated filament, and in particular a flip of its chirality. This was modeled in a biophysical study for the bacterium *Rhodobacter sphaeroides* with two different polymorphs (Vogel & Stark, 2013). Similar chirality transformations have been obtained in the lab using tethered flagella in external flows (Coombs et al., 2002; Hotani, 1982). A helical flagellum held in a uniform stream is subject to a flow-induced tension as well as hydrodynamic moments, which are able to induce chirality reversal and cyclic transfor-

mations between right (curly or semi-coiled) and left-handed (normal) helices.

One aspect of polymorphism where fluid dynamics plays a fascinating role is the propulsive performance of each flagellar waveforms. For each waveform, an intrinsic propulsive efficiency may be defined from the mobility matrix of the helix, comparing the power used for locomotion to the power expended by the rotary motor against the fluid (Purcell, 1997). Physically, efficient helices are those which maximize the propulsive coupling between rotation and translation while minimizing the resistance in both translation and rotation. A near-rod helix, such as polymorph #9 in Fig. 5a, or one with a small wavelength, such as polymorph #3, will be very inefficient. Which one of the different shapes is the most efficient? This is illustrated in Fig. 5b which plots the isovalues of the intrinsic hydrodynamic efficiency as a function of the helix wavelength and the circumference of the cylinder on which it is coiled (Spagnolie & Lauga, 2011). Left-handed (resp. right-handed) helices are denoted with negative (resp. positive) wavelengths. Superimposed on the color map are the geometrical measurements from the actual polymorphs for peritrichous (black symbols) and polar flagella (blue symbols) together with the theoretical shapes predicted by molecular theories (red symbols) (Calladine, 1978). Filled (resp. empty) symbols refer to the left-handed (resp. right-handed) polymorphs shown in Fig. 5a. The two circles allow one to distinguish between peritrichous and polar polymorphs. In all cases, the most efficient waveform is the left-handed normal polymorph (#2 in Fig. 5a). This is the waveform displayed by bacteria during forward locomotion. Further,

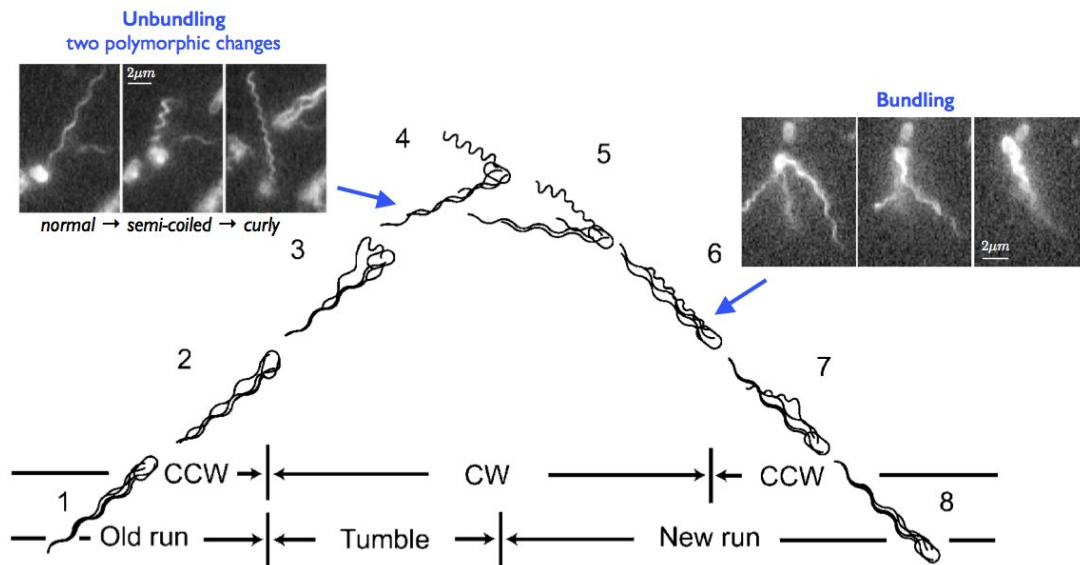


FIG. 6 A run-to-tumble-to-run transition for swimming *E. coli* as a model for the reorientation mechanism of peritrichous bacteria (Darnton et al., 2007; Turner et al., 2000). During a run all motors turn CCW while in a tumble at least one motor turns CW which induces polymorphic changes in the associated flagellar filament, typically from normal to semi-coiled and then curly (unbundling) before returning to the normal shape at the beginning of a new run (bundling). All figures reproduced with permission.

not only is the normal helix the most efficient among all polymorphs, it is in fact close to being the overall optimal (which is at the intersection of the black circles and the warm color in the map). In addition, further analysis of the results reveals that the second and third most efficient waveforms are the right-handed semi-coiled (#4 in Fig. 5a) and curly (#5), both of which are the waveforms used by wild-type swimming bacteria to change directions (see §VI). These results suggest that fluid dynamics and mechanical efficiencies might have provided strong physical constraints in the evolution of bacterial flagella.

VI. HYDRODYNAMICS OF REORIENTATIONS

Swimming is the mechanism which allows bacteria to sample their environment (Purcell, 1977). Because they are small, bacteria are not able to sustain directional swimming for extended periods of time, and as a consequence they always display diffusive behavior at long times. For swimming at speed U for a time τ followed by a random change of direction, the long-time behavior is diffusive, $r^2 \sim Dt$ with the diffusivity scaling as $D \sim U^2\tau$, typically much larger than Brownian diffusivities (Berg, 1993). When this diffusive dynamics is biased using sensing from the cells of their chemical environment, it leads to net drift and chemotaxis (Berg, 2004; Schnitzer, 1993).

While the value of U is dictated by the hydrodynamics of swimming, what sets the time scale τ and how

do cells manage to reorient? The time scale is set internally by the sensing apparatus of bacteria, a complex but well-characterized internal protein network which chemically links the information gathered by receptors on the cell membrane to the action of the rotary motor (Falke et al., 1997). In order for the cells to then reorient, three mechanisms have been discovered, each taking advantage of different physics, and each involving fluid dynamics (Mitchell, 2002).

The first one is termed run-and-stop, where a bacterium swims and then stops, simply waiting for thermal noise to reorient the cell. The time scale is therefore set in this case by a balance between the magnitude of thermal noise and the viscous mobility of the whole cell in rotation, leading to reorientation times on the order of seconds. The second mechanism, termed run-and-reverse, is used by many polar marine bacteria (Stocker & Seymour, 2012). In that case, the rotary motor alternates between CCW and CW rotations. Kinematic reversibility for the surrounding fluid would predict that by doing so the cells should keep retracing their steps. However, the propulsive forcing from the fluid on the flagellar filament, which is transmitted to the flexible hook, is able to induce buckling of the hook which leads to a random reorientation of the cell, thereby escaping the reversibility argument (Son et al., 2013; Xie et al., 2011).

The third, and most-studied, mechanism is called run-and-tumble, used by peritrichous bacteria such as *E. coli*, and whose details were made clear by a pioneering experiment allowing to visualize flagellar filaments in real time (Turner et al., 2000) (see illustration in Fig. 6). Criti-

cal to the effective locomotion in this case is the ability of multiple flagellar filaments to bundle when they all rotate in the same direction, and unbundle otherwise (Macnab, 1977; Magariyama et al., 2001). When a bacterium runs, all its flagellar filaments adopt the normal waveform, turn in a CCW fashion (when viewed from behind the cell looking in), and are gathered in a tight, synchronized helical bundle behind the cell. Based on chemical clues from its environment, the cell might then initiate a tumbling event (which is Poisson distributed), for which at least one motor (but possibly more) switches its direction rotation to CW, inducing a polymorphic change of its flagellar filament from normal to semi-coiled (in most cases) which at the same time flies out of the bundle, resulting in a change of orientation for the cell body. As the motor continues to rotate CW, the flagellum switches to the curly shape, and then when the motor reverts back to a CCW rotation, comes back to the normal shape and returns into the bundle. These short tumbles typically last $\tau \sim 0.1s$ while the runs last about one second. Note that many mutants of *E. coli* exist, either naturally occurring or genetically induced in the lab, displaying some variation in geometry or behavior; for example, the mutant HCB-437 does not tumble and is smooth swimming (Wolfe et al., 1988).

The bundling and unbundling of flagellar filaments compose a large-deformation fluid-structure interaction problem at low Reynolds numbers combined with short-range flagella-flagella electrostatic repulsion (Lytle et al., 2002; Weibull, 1950). Due to this complexity, physical studies of bundling have taken two drastically different approaches. On one hand, investigations have been carried out on very simplified geometries and setups, either numerically (Kim & Powers, 2004; Reichert & Stark, 2005) or experimentally at the macroscopic scale (Kim et al., 2003; Macnab, 1977; Qian et al., 2009), in order to probe synchronization between driven identical helices and their bundling. It was found that nonlocal hydrodynamic interactions between helices were sufficient to induce attraction, wrapping, and synchronization provided the helices were of the right combination of chirality (both left-handed and rotating CCW or their mirror-image equivalent) but some amount of elastic compliance was required. Biologically, it was argued that this flexibility could be provided by the hook.

On the other hand, some groups have attempted to tackle the complexity of the problem using realistic setups of deforming flagellar filaments from various (often formidable) computational angles, including the use of regularized flow singularities (Flores et al., 2005), the immersed boundary method (Lim & Peskin, 2012), mesoscale methods (Reigh et al., 2012), boundary elements (Kanehl & Ishikawa, 2014) and bead-spring models adapted from polymer physics (Janssen & Graham, 2011; Watari & Larson, 2010). The numerical results confirm the physical picture of bundling and unbundling driven by a combination of flexibility and hydrodynamic interactions, with a critical dependence on the geometri-

cal details, the relative configuration of the flagella, and the value of the motor torques driving the rotation.

VII. BACTERIA SWIMMING NEAR SURFACES

Surfaces are known to affect the behavior of bacteria (Harshey, 2003; Vanloosdrecht et al., 1990). One of the most striking aspect of locomotion near boundaries is the tendency of swimming bacteria to be attracted to surfaces, with steady-state concentration showing 10 fold-increases near surfaces (Berke et al., 2008). This is illustrated in Fig. 7a for smooth-swimming (i.e. non-tumbling) *E. coli* cells. The attraction mechanism was first argued to be purely hydrodynamic in nature (Berke et al., 2008; Hernandez-Ortiz et al., 2005), easily understood as an image effect. As seen in §IV, the flow perturbation induced by a swimming bacterium is (at leading order in the far field) a pusher force dipole. The hydrodynamic image system necessary to enforce a no-slip boundary condition on a flat surface includes a force dipole, a force quadrupole, and a source dipole, all located on the other side of the surface (purple arrows in Fig. 7b) (Blake, 1971). The net effect of these image singularities on the original dipole is an hydrodynamic attraction toward the wall (black arrow). Intuitively, a pusher dipole draws fluid in from its side, and therefore pulls itself toward a surface when swimming parallel to it. Similarly, the hydrodynamic moment induced by the image system is able to rotate pusher dipoles so that their stable orientation is swimming parallel to the surface (Berke et al., 2008), leading to kinematic asymmetries for bacteria switching between pusher and puller modes (Magariyama et al., 2005).

Experimental measurements of the flow induced by bacteria showed, however, that this dipolar flow gets quickly overwhelmed by noise a few cell lengths away, and thus acts only when the cells are close to the surface, leading to long residence times (Drescher et al., 2011). For cells which swim toward a surface and get trapped there, what determines the long-time equilibrium distance between swimming cells and surfaces, and their orientation? Although simple models all predict bacteria eventually touching walls and therefore require short-range repulsion (Dunstan et al., 2012; Spagnolie & Lauga, 2012), boundary element computations with a model polar bacterium demonstrated that hydrodynamics alone was able to select a stable orbit with swimming at a finite distance (Fig. 7c) (Giacché et al., 2010).

A second remarkable feature of bacteria swimming near surface is a qualitative change in their trajectories. Between reorientation events, flagellated bacteria far from walls swim along straight or wiggly paths. Near rigid surfaces, their trajectories are observed to become circular, typically CW when viewed from above the surface in the fluid (Berg & Turner, 1990; Frymier et al., 1995). This is illustrated in Fig. 7d for an individually-tracked *E. coli* cell swimming near a glass surface (Vigeant

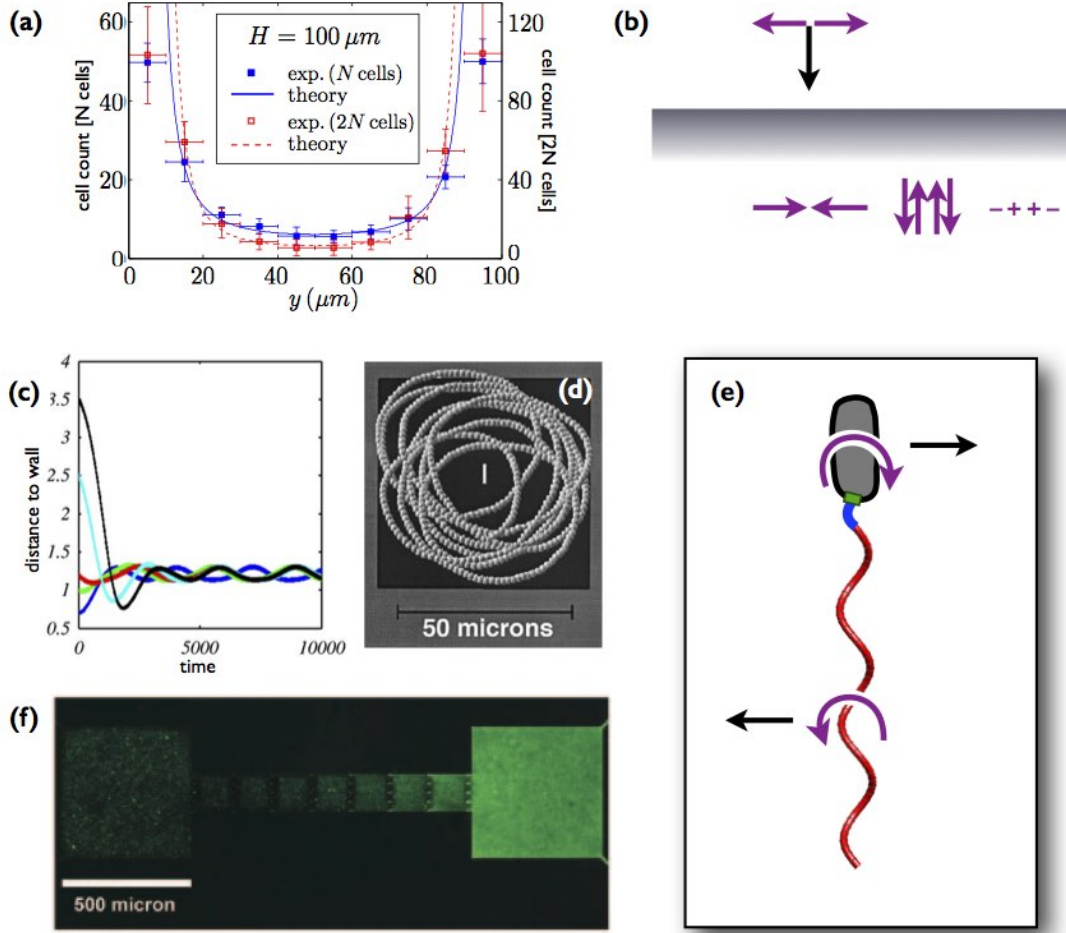


FIG. 7 (a) Attraction of smooth-swimming *E. coli* cells by two rigid surfaces located at $y = 0$ and $y = 100 \mu\text{m}$ (symbols) and fit by a point-dipole model (lines) (Berke et al., 2008); (b) Hydrodynamic images for a pusher force dipole above a flat no-slip surface (purple arrows) leading to attraction by the surface (black arrow); (c) Computations showing stable swimming at a finite distance from a rigid surface for a polar bacterium (distance to wall nondimensionalized by cell size as a function of time nondimensionalized by flagellar rotational frequency) (Giacché et al., 2010); (d) Tracking data for a smooth-swimming *E. coli* cell near a glass surface (Vigeant & Ford, 1997); (e) Physical interpretation of wall-induced moment on bacterium with helical flagellar filament leading to circular swimming: the rotating flagellum is subject to a surface-induced force to its left (when viewed from above) and the counter-rotating body by a force in the opposite direction, leading to a moment and therefore rotation of the cell; (f) Rectification of fluorescent swimming *E. coli* in channels with asymmetric geometrical features (Galajda et al., 2007). All figures reproduced with permission.

& Ford, 1997). Early computations for model polar bacteria also predicted circular trajectories (Ramia et al., 1993) while recent experiments showed that the physicochemical nature of the interface plays a critical role selecting the rotation direction (Lemelle et al., 2013; Morse et al., 2013).

The switch from forward to circular swimming is a fluid dynamics effect owing to new forces and moments induced near surfaces (Lauga et al., 2006). This is illustrated in Fig. 7e for locomotion of model polar bacterium above of a rigid wall. A helix rotating parallel to a no-slip surface is subject to a net force whose direction depends on the chirality of the helix and its direction of rotation

(to the left in Fig. 7d for a CCW rotation of a left-handed helix). Similarly, as the cell body is counter-rotating, it is subject to a hydrodynamic force in the direction of its rolling motion on the surface (to the right in Fig. 7d) (Kim & Karrila, 1991). These two forces are exactly zero far from the surface and their magnitudes depend strongly on the distance to the wall (Li et al., 2008). The net effect of these forces is a wall-induced moment acting on the cell. Since the cell is torque-free, it needs to rotate (here, CW when viewed from above), leading to circular trajectories. Notably, the sign of the surface-induced forces are reversed if the rigid wall is replaced by a free surface, leading to circular swimming in the oppo-

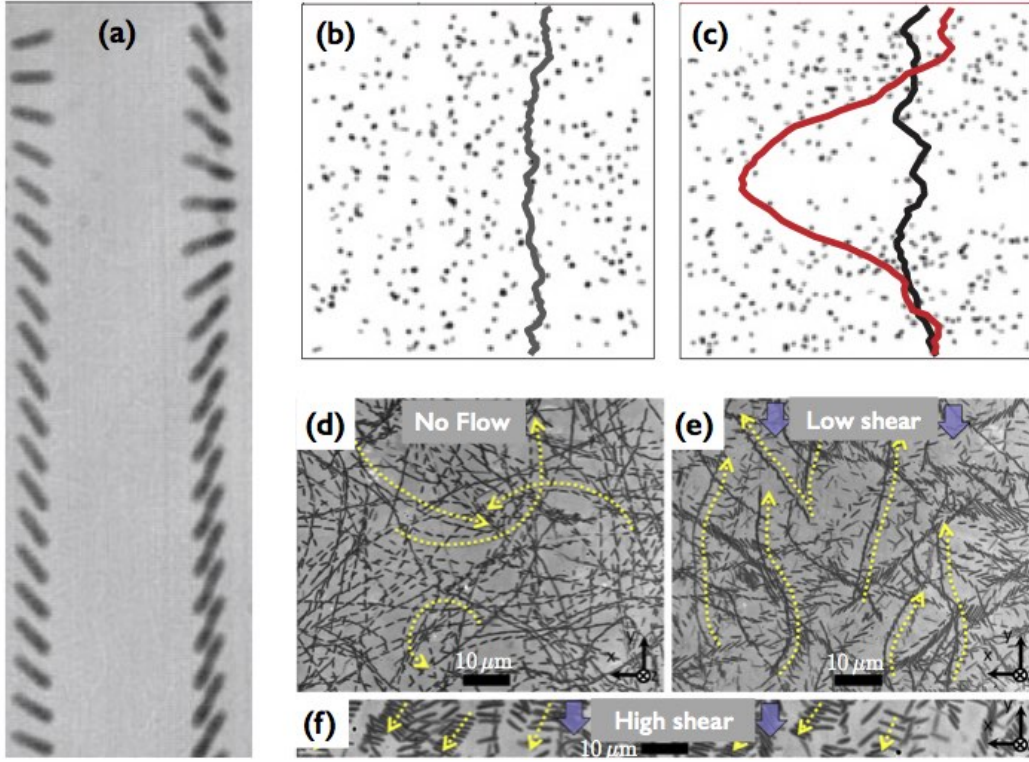


FIG. 8 (a) Jeffery's orbits for non-flagellated *E. coli* cells in a microchannel (Kaya & Koser, 2009); (b) Non-motile *Bacillus subtilis* cells show a uniform concentration under non-uniform shear (Rusconi et al., 2014); (c) Motile cells initially uniformly distributed (black line) accumulate under non-uniform shear in the high-shear regions (red line); (d) Motile *E. coli* cells swimming in circles near rigid surfaces in the absence of flow (Kaya & Koser, 2012); (e) Upstream swimming of the same cells under moderate shear; (f) Under strong shear, all cells are advected downstream. All figures reproduced with permission.

site direction (Di Leonardo et al., 2011), and a possible co-existence between CW and CCW for cell populations near complex interfaces (Lemelle et al., 2013; Lopez & Lauga, 2014; Morse et al., 2013).

The interactions of bacteria with complex geometries have also lead to fascinating results. Swimming *E. coli* cells in rectangular microchannels with three polymeric walls and one agar surface showed a strong preference to swim near the agar side of the channels (DiLuzio et al., 2005), a phenomenon still unexplained. The same bacteria are rectified by channels with asymmetric geometrical features (Galajda et al., 2007), which can then be exploited to passively increase cell concentrations (Fig. 7f). Similarly, bacteria can be harnessed to perform mechanical work and, for example, rotate asymmetric microgears (Di Leonardo et al., 2010; Sokolov et al., 2010). In strong confinement, helical flagella continue to induce propulsion, but the swimming speed decreases for motion driven at constant torque (Liu et al., 2014a). Related experiments show that the limit of flagella-driven motility is reached when the cell body has clearance of about less than 30% of its size, although cells can continue to move in smaller channels through cell division (Männik et al., 2009).

VIII. BACTERIA IN FLOWS

Similarly to colloidal particles, swimming bacteria respond to external flows by being passively advected and rotated. In many relevant situations where the cells are much smaller than any of the flow length scales (e.g. in marine environments), the flow can be assumed to be locally linear, and thus a superposition of uniform translation, pure extension, and pure rotation. In that case, the dynamics of the (elongated) bacteria is described by Jeffery's equation which is exact for prolate spheroids in linear flows (Pedley & Kessler, 1992). Physically, the cells move with the mean flow velocity and their rotation rate is the sum of the vorticity component (which alone would predict rotation at a constant rate) and the (potential) extensional component (which alone would predict steady alignment with the principal axis of extension). The resulting tumbling trajectories, called Jeffery's orbits, are illustrated in Fig. 8a for non flagellated *E. coli* cells under shear in a microfluidic device (Kaya & Koser, 2009).

In addition to the classical Jeffery's orbits, bacteria are subject to an additional mechanism which results from their chiral shapes. The hydrodynamics of a helical flagellum in a simple shear flow leads to a viscous torque be-

ing produced on the helix, which reorients it away from the plane of shear. Combined with motility, this is an example of *rheotaxis* where cells respond to shear (here, purely physically) (Marcos et al., 2012). Beyond the assumption of linear flow, swimming bacteria respond to non-uniform shears by developing non-uniform orientation distributions, which, when coupled to motility, lead to cells accumulating in the high shear regions (Rusconi et al., 2014). This is illustrated in Fig. 8b-c for *Bacillus subtilis* in Poiseuille flow. Non-swimming cells have a uniform distribution (Fig. 8b) whereas motile cells starting uniformly distributed (black line in Fig. 8c) develop non-uniform distributions and gather in the high-shear regions (red line Fig. 8c).

One compelling aspect of the response of bacteria to external flows is the feedback of swimming cells on the surrounding fluid through the stresses they exert. Due to their dipolar flows, swimming bacteria exert bulk stresses on the fluid – hence the term “stresslet” originally coined by Batchelor in the context of passive suspensions (Batchelor, 1970). A group of swimming bacteria subject to an external deformation will thus generically respond by a state of stress with a rich dynamics. The most fundamental question relating stresses to deformation in the fluid is: what is the effective viscosity of a suspension of swimming bacteria? Experiments have been first carried out with the peritrichous *Bacillus subtilis* by estimating the viscosity in two different ways, first by looking at the unsteady decay of vortex and then by measuring directly the torque on a rotating probe in the cell suspension (Sokolov & Aranson, 2009). The results showed a strong reduction in the effective viscosity (up to a factor of seven), while an increase was possible at larger cell concentrations. A different setup was proposed for *E. coli* where a suspension was flown in a microchannel and the effective viscosity estimated using predictions for the unidirectional flow profile from multiphase Newtonian fluid dynamics (Gachelin et al., 2013). In that case, the effective viscosity showed an initial decrease, followed by shear-thickening up to relative viscosities above 1, followed by shear-thinning at high shear rates. In parallel, theoretical and computational work on model cells in both shear and extensional flows predicted the viscosity decrease for pusher cells, together with the possibility of negative viscosities and normal stress coefficients of sign opposite to the ones for passive suspensions (Haines et al., 2009; Saintillan, 2010a,b).

Finally, bacteria swimming near boundaries in external flows also have a propensity to swim upstream and hence against the flow (Cisneros et al., 2007; Hill et al., 2007). This is illustrated in Fig. 8d-f where motile *E. coli* cells which swim in circles in the absence of flow (Fig. 8d) are seen to move upstream under moderate shear (Fig. 8e) and are passively advected downstream at high shear (Fig. 8f) (Kaya & Koser, 2012). The physical origin of this transition to upstream swimming has been proposed to be hydrodynamic, whereby a shear flow of moderate strength produces a torque on a downward-facing

cell which reorients it so that its stable equilibrium is to point upstream and thus swim against the flow (Hill et al., 2007; Kaya & Koser, 2012).

IX. LOCOMOTION IN COMPLEX FLUIDS

Bacteria who inhabit soils and higher organisms routinely have to progress through complex environments with microstructures whose characteristic length scales might be similar to that of the cell. Some bacteria also have to endure chemically- and mechanically-heterogeneous environments. For example, *Helicobacter pylori*, which survives in the acidic environment of the stomach, creates an enzyme which locally increases pH and can induce rheological changes to the mucus protecting the epithelium surface of the stomach, changing it from a gel to a viscous fluid in which it is able to swim (Bansil et al., 2013). In many instances, the surrounding fluids might not be totally flowing but instead possess their own relaxation dynamics, which might occur on time scales comparable to the intrinsic time scales of the locomotion. For example, during biofilm formation, bacteria produce an extracellular polymeric matrix for which they control the mechanical properties through water content (Costerton et al., 1995; Wilking et al., 2011) (Fig. 9a). A number of studies have attempted to quantify the impact of such complex fluids on the swimming kinematics and energetics of bacteria.

Early studies were concerned with perhaps the simplest question possible: How is bacterial locomotion modified by a change in the viscosity of the surrounding (Newtonian) fluid? Flagellated bacteria display a systematic two-phase response, where an increase in viscosity is seen to first lead to a small increase in the swimming speed followed by a sharp decrease at large viscosities (Greenberg & Canale-Parola, 1977; Schneider & Doetsch, 1974; Shoesmith, 1960). The decrease has been rationalized by assuming that the rotary motor is working at constant power output (Keller, 1974), an assumption we now know is erroneous since it is the motor torque which is constant (see §II). In stark contrast with flagellated bacteria, spirochetes show a systematic enhancement of their swimming speed with an increase of the viscosity of the fluid (Kaiser & Doetsch, 1975). In a related study, the viscosity required to immobilize bacteria was measured to be larger, by orders of magnitude, for spirochetes compared to flagellated bacteria (Greenberg & Canale-Parola, 1977).

How can the difference between flagellated bacteria and spirochetes be rationalized? One argument brought forward focused on the details of the microstructure of the fluid, arguing that all increases in viscosity are not created equal (Berg & Turner, 1979). Increases in viscosity are induced by dissolving polymers, but the nature of the polymer chains structure may be critical. Experiments showing large increases in swimming speeds used solution of long unbranched chain polymers (e.g., methyl-

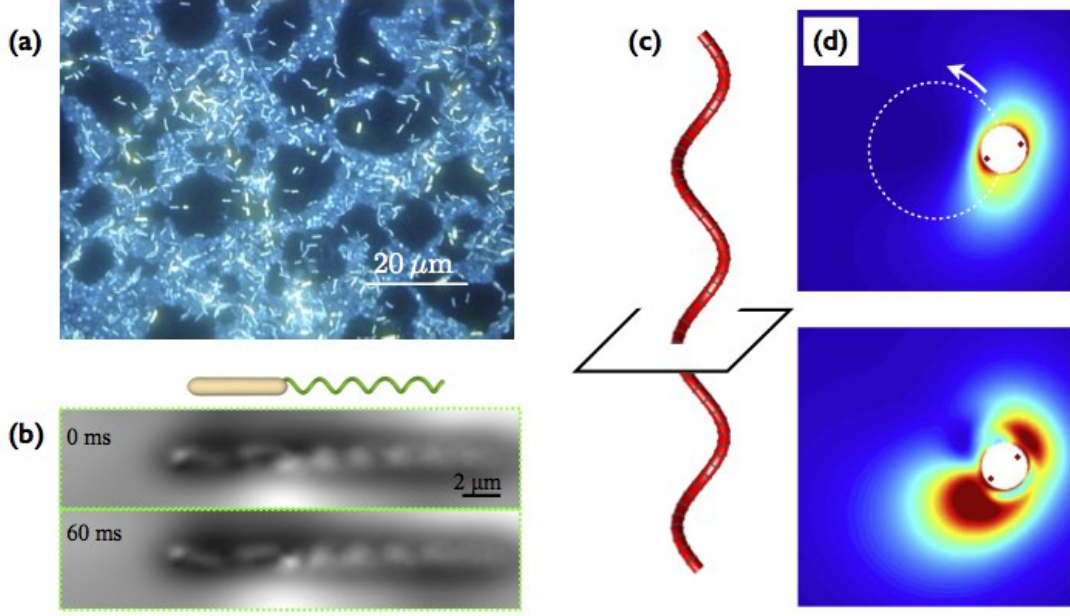


FIG. 9 (a) Biofilm on the stainless steel surface of a bioreactor (Centers for Disease Control and Prevention); (b) Waves in the director field created by rotating flagella of the peritrichous *B. subtilis* in a liquid crystal (Zhou et al., 2014); (c-d) Magnitude of the polymer stresses in the cross section of a flagellum rotating in a Oldroyd-B fluid (nondimensionalized by the viscosity times the filament rotation rate) from computations (the white dashed line indicates the path followed by the flagellum centerline) (Spagnolie et al., 2013). Top: $De = 0.3$; bottom: $De = 1.5$. All figures reproduced with permission.

cellulose) which are expected to form a network against which the cells are effectively able to push. In contrast, solutions of branched polymers are more homogeneous, and should lead to a decrease of the swimming speed since, for a constant-torque motor rotating in a viscous fluid, the product of the viscosity by the rotational frequency needs to remain constant. The idea that the presence of the microstructure itself in the solvent is critical in explaining the change in swimming speeds was further modeled mathematically, with a similar physical picture (Leshansky, 2009; Magariyama & Kudo, 2002). Recent experiments further shed light on the interplay between the viscosity of the fluid and the torque applied by the rotary motor (Martinez et al., 2014). If the fluid is anisotropic (for example a liquid crystal), a strong coupling can develop between the director field and the bacteria, enabling constrained locomotion and fascinating novel flow features with truly long-ranged interactions (Fig. 9b) (Zhou et al., 2014).

Recent work has focused on viscoelastic fluids with the primary motivation to understand the locomotion of bacteria, and higher organisms, in mucus (Lauga, 2014). Such fluids have the added complexity of having finite relaxation times, λ , and for flagella rotating with frequency ω a dimensionless Deborah number, $De = \lambda\omega$, needs to be considered. Small-amplitude theory on flagellar propulsion predicted that the relaxation in the fluid would always leads to slower swimming (Fu et al., 2007; Lauga, 2007). Experiments with macroscopic helices driven in

rotation and undergoing force-free translation confirmed the small-amplitude theoretical results but showed that helices with larger amplitudes could experience a moderate increase in translational speed for order one Deborah numbers (Liu et al., 2011). Detailed numerics on the same setup argued that the increase was due to the rotating flagellum revisiting its viscoelastic wake, as illustrated in Fig. 9c-d for $De = 0.3$ (top) and $De = 1.5$ (bottom) (Spagnolie et al., 2013).

X. SUMMARY POINTS

1. Low-Reynolds-number hydrodynamics is at the heart of the fundamental physics of bacteria swimming, first and foremost by the generation of propulsive forces. It might have also played a role in the evolution of the bacterial flagellum resulting in optimal polymorphic shapes used for forward motion.
2. At the level of a single-cell, fluid dynamic forces are exploited by peritrichous bacteria to induce fast bundling and unbundling of their multiple flagella, resulting in efficient reorientation mechanisms.
3. The flows created by swimming bacteria affect the interactions with their environment and with other cells leading to enhanced nutrient transport

and collective locomotion. Similarly, complex microstructures or external flows can have significant influence on the trajectories, concentrations, and orientations of swimming bacteria.

4. Although surrounding fluids play important roles in the life of bacteria, hydrodynamic forces on flagellar filaments and cell bodies often have to be balanced with bending and twisting elasticity, short-range electrostatic interactions, and are subject to both biochemical and thermal noise. Fluid dynamics is therefore only one of the complex physical processes at play.

XI. FUTURE ISSUES

1. Why is the value of the experimentally-measured torque applied by the rotary motor so different from that from hydrodynamic predictions (Darnnton et al., 2007)? What are the other mechanical forces at play?
2. Why does the flagellar hook of peritrichous bacteria not buckle, as it does for polar bacteria under seemingly similar propulsive conditions (Son et al., 2013)? Why is the flagellar hook so precisely tuned in size and rigidity that flagellar bundling is no longer possible if small changes are made to it (Brown et al., 2012)?
3. How exactly can a tight bundle of multiple flagella open up and close repeatedly without jamming under the uncoordinated action of a few motors (Macnab, 1977)? How much of this process is truly driven by hydrodynamic interactions vs. other passive mechanisms?
4. Can we derive predictive whole-cell models able to reproduce the full run-and-tumble statistics of swimming bacteria based solely on our understanding on the behavior of rotary motors (Turner et al., 2000)?

Acknowledgements

I thank Tom Montenegro-Johnson for his help with the figures. Discussions with Howard Berg and Ray Goldstein are gratefully acknowledged. This work was funded in part by the European Union (through a Marie-Curie CIG Grant) and by the Isaac Newton Trust (Cambridge).

References

- Allen RD, Baumann P. 1971. Structure and arrangement of flagella in species of the genus *Beneckea* and *Photobacterium fischeri*. *J. Bacteriol.* 107:295–302
- Bansil R, Celli JP, Hardcastle JM, Turner BS. 2013. The influence of mucus microstructure and rheology in *Helicobacter pylori* infection. *Front. Immun.* 4:310
- Batchelor GK. 1970. The stress system in a suspension of force-free particles. *J. Fluid Mech.* 41:545–570
- Berg HC. 1993. *Random Walks in Biology*. New Jersey: Princeton University Press
- Berg HC. 2003. The rotary motor of bacterial flagella. *Annu. Rev. Biochem.* 72:19–54
- Berg HC. 2004. *E. coli in Motion*. New York, NY: Springer-Verlag
- Berg HC, Anderson RA. 1973. Bacteria swim by rotating their flagellar filaments. *Nature* 245:380–382
- Berg HC, Turner L. 1979. Movement of microorganisms in viscous environments. *Nature* 278:349–351
- Berg HC, Turner L. 1990. Chemotaxis of bacteria in glass capillary arrays – *Escherichia coli*, motility, microchannel plate, and light scattering. *Biophys. J.* 58:919–930
- Berke AP, Turner L, Berg HC, Lauga E. 2008. Hydrodynamic attraction of swimming microorganisms by surfaces. *Phys. Rev. Lett.* 101:038102
- Berry RM, Berg HC. 1997. Absence of a barrier to backwards rotation of the bacterial flagellar motor demonstrated with optical tweezers. *Proc. Natl. Acad. Sci., USA* 94:14433–14437
- Blair DF. 1995. How bacteria sense and swim. *Annu. Rev. Microbiol.* 49:489–520
- Blake JR. 1971. A note on the image system for a stokeslet in a no-slip boundary. *Proc. Camb. Phil. Soc.* 70:303–310
- Bray D. 2000. *Cell Movements*. New York, NY: Garland Publishing
- Brennen C, Winet H. 1977. Fluid mechanics of propulsion by cilia and flagella. *Annu. Rev. Fluid Mech.* 9:339–398
- Brown MT, Steel BC, Silvestrin C, Wilkinson DA, Delalez NJ, et al. 2012. Flagellar hook flexibility is essential for bundle formation in swimming *Escherichia coli* cells. *J. Bacter.* 194:3495–3501
- Calladine CR. 1978. Change of waveform in bacterial flagella : the role of mechanics at the molecular level. *J. Mol. Biol.* 118:457–479
- Chattopadhyay S, Moldovan R, Yeung C, Wu XL. 2006. Swimming efficiency of bacterium *Escherichia coli*. *Proc. Natl. Acad. Sci. USA* 103:13712–13717
- Chattopadhyay S, Wu X. 2009. The effect of long-range hydrodynamic interaction on the swimming of a single bacterium. *Biophys. J.* 96:2023–2028
- Chen X, Berg HC. 2000. Torque-speed relationship of the flagellar rotary motor of *Escherichia coli*. *Biophys. J.* 78:1036–1041
- Chwang AT, Wu TY. 1971. Helical movement of microorganisms. *Proc. Roy. Soc. Lond. B* 178:327–346
- Chwang AT, Wu TY. 1975. Hydromechanics of low-Reynolds-number flow. Part 2. Singularity method for Stokes flows. *J. Fluid Mech.* 67:787–815
- Chwang AT, Wu TY, Winet H. 1972. Locomotion of *spirilla*. *Biophys. J.* 12:1549
- Cisneros LH, Cortez R, Dombrowski C, Goldstein RE, Kessler JO. 2007. Fluid dynamics of self-propelled microorganisms, from individuals to concentrated populations. *Exp. Fluids* 43:737–753
- Coombs D, Huber G, Kessler JO, Goldstein RE. 2002. Periodic chirality transformations propagating on bacterial flagella. *Phys. Rev. Lett.* 89:118102–1–118102–4
- Copeland MF, Weibel DB. 2009. Bacterial swarming: a model

- system for studying dynamic self-assembly. *Soft Matt.* 5:1174–1187
- Costerton JW, Lewandowski Z, Caldwell DE, Korber DR, Lappinscott HM. 1995. Microbial biofilms. *Annu. Rev. Microbiol.* 49:711–745
- Cox RG. 1970. The motion of long slender bodies in a viscous fluid. Part 1. General theory. *J. Fluid Mech.* 44:791–810
- Darnton NC, Berg HC. 2007. Force-extension measurements on bacterial flagella: Triggering polymorphic transformations. *Biophys. J.* 92:2230–2236
- Darnton NC, Turner L, Rojevsky S, Berg HC. 2007. On torque and tumbling in swimming *Escherichia coli*. *J. Bacteriol.* 189:1756–1764
- Darnton NC, Turner L, Rojevsky S, Berg HC. 2010. Dynamics of bacterial swarming. *Biophys. J.* 98:2082–2090
- Di Leonardo R, Angelani L, DellArciprete D, Ruocco G, Iebba V, et al. 2010. Bacterial ratchet motors. *Proc. Natl. Acad. Sci. U.S.A.* 107:9541–9545
- Di Leonardo R, Dell’Arciprete D, Angelani L, Iebba V. 2011. Swimming with an image. *Phys. Rev. Lett.* 106:038101
- DiLuzio WR, Turner L, Mayer M, Garstecki P, Weibel DB, et al. 2005. *Escherichia coli* swim on the right-hand side. *Nature* 435:1271–1274
- Doi M, Edwards SF. 1988. *The Theory of Polymer Dynamics*. Oxford, U.K.: Oxford University Press
- Drescher K, Dunkel J, Cisneros LH, Ganguly S, Goldstein RE. 2011. Fluid dynamics and noise in bacterial cell-cell and cell-surface scattering. *Proc. Natl. Acad. Sci. U.S.A.* 108:10940–10945
- Dunstan J, Miño G, Clement E, Soto R. 2012. A two-sphere model for bacteria swimming near solid surfaces. *Phys. Fluids* 24:011901
- Ehlers K, Oster G. 2012. On the mysterious propulsion of *Synechococcus*. *PLOS One* 7:e36081
- Falke JJ, Bass RB, Butler SL, Chervitz SA, Danielson MA. 1997. The two-component signaling pathway of bacterial chemotaxis: A molecular view of signal transduction by receptors, kinases, and adaptation enzymes. *Annu. Rev. Cell Dev. Biol.* 13:457
- Fauci LJ, Dillon R. 2006. Biofluidmechanics of reproduction. *Annu. Rev. Fluid Mech.* 38:371–394
- Flores H, Lobaton E, Mendez-Diez S, Tlupova S, Cortez R. 2005. A study of bacterial flagellar bundling. *Bull. Math. Biol.* 67:137–168
- Frymier PD, Ford RM, Berg HC, Cummings PT. 1995. Three-dimensional tracking of motile bacteria near a solid planar surface. *Proc. Natl. Acad. Sci. USA* 92:6195–6199
- Fu HC, Powers TR, Wolgemuth HC. 2007. Theory of swimming filaments in viscoelastic media. *Phys. Rev. Lett.* 99:258101–258105
- Fujii M, Shibata S, Aizawa SI. 2008. Polar, peritrichous, and lateral flagella belong to three distinguishable flagellar families. *J. Mol. Biol.* 379:273–283
- Gachelin J, Miño G, Berthet H, Lindner A, Rousselet A, Clément E. 2013. Non-newtonian viscosity of *Escherichia coli* suspensions. *Phys. Rev. Lett.* 110:268103
- Gaffney EA, Gadelha H, Smith DJ, Blake JR, Kirkman-Brown JC. 2011. Mammalian sperm motility: Observation and theory. *Annu. Rev. Fluid Mech.* 43:501–528
- Galajda P, Keymer JE, Chaikin P, Austin RH. 2007. A wall of funnels concentrates swimming bacteria. *J. Bacteriol.* 189:8704–8707
- Ghosh A, Fischer P. 2009. Controlled propulsion of artificial magnetic nanostructured propellers. *Nano Lett.* 9:2243–2245
- Giacché D, Ishikawa T, Yamaguchi T. 2010. Hydrodynamic entrapment of bacteria swimming near a solid surface. *Phys. Rev. E* 82:056309
- Goldstein RE. 2015. Green algae as model organisms for biological fluid dynamics. *Annu. Rev. Fluid Mech.* 47:34375
- Goldstein SF, Buttke KF, Charon NW. 1996. Structural analysis of the *Leptospiraceae* and *Borrelia burgdorferi* by high-voltage electron microscopy. *J. Bacteriol.* 178:6539–6545
- Gray J, Hancock GJ. 1955. The propulsion of *Sea-urchin* spermatozoa. *J. Exp. Biol.* 32:802–814
- Greenberg EP, Canale-Parola E. 1977. Motility of flagellated bacteria in viscous environments. *J. Bacteriol.* 132:356–358
- Guasto JS, Rusconi R, Stocker R. 2012. Fluid mechanics of planktonic microorganisms. *Annu. Rev. Fluid Mech.* 44:373400
- Haines BM, Sokolov A, Aranson IS, Berlyand L, Karpeev DA. 2009. Three-dimensional model for the effective viscosity of bacterial suspensions. *Phys. Rev. E* 80:041922
- Hancock GJ. 1953. The self-propulsion of microscopic organisms through liquids. *Proc. Roy. Soc. Lond. A* 217:96–121
- Harshey RM. 2003. Bacterial motility on a surface: Many ways to a common goal. *Annu. Rev. Microbiol.* 57:249–273
- Hasegawa K, Yamashita I, Namba K. 1998. Quasi- and nonequivalence in the structure of bacterial flagellar filament. *Biophys. J.* 74:569–575
- Hernandez-Ortiz JP, Stoltz CG, Graham MD. 2005. Transport and collective dynamics in suspensions of confined swimming particles. *Phys. Rev. Lett.* 95:204501
- Higdon JLL. 1979. Hydrodynamics of flagellar propulsion – Helical waves. *J. Fluid Mech.* 94:331–351
- Hill J, Kalkanci O, McMurtry JL, Koser H. 2007. Hydrodynamic surface interactions enable *Escherichia coli* to seek efficient routes to swim upstream. *Phys. Rev. Lett.* 98:1–4
- Hotani H. 1980. Micro-video study of moving bacterial flagellar filaments. II. Polymorphic transition in alcohol. *Biosyst.* 12:325–330
- Hotani H. 1982. Micro-video study of moving bacterial flagellar filaments III. Cyclic transformation induced by mechanical force. *J. Mol. Biol.* 156:791
- Hyon Y, Marcos, Powers TR, Stocker R, Fu HC. 2012. The wiggling trajectories of bacteria. *J. Fluid Mech.* 705:58–76
- Imhoff JF, Trüper HG. 1977. *Ectothiorhodospira halochloris* sp. nov., a new extremely halophilic phototrophic bacterium containing bacteriochlorophyll b*. *Arch. Microbiol.* 114:115–121
- Ishikawa T, Sekiya G, Imai Y, Yamaguchi T. 2007. Hydrodynamic interaction between two swimming bacteria. *Biophys. J.* 93:2217–2225
- Janssen PJA, Graham MD. 2011. Coexistence of tight and loose bundled states in a model of bacterial flagellar dynamics. *Phys. Rev. E* 84
- Jarrell KF, McBride MJ. 2008. The surprisingly diverse ways that prokaryotes move. *Nature Rev. Microbiol.* 6:466–476
- Johnson RE. 1980. An improved slender body theory for Stokes flow. *J. Fluid Mech.* 99:411–431
- Johnson RE, Brokaw CJ. 1979. Flagellar hydrodynamics. a comparison between resistive-force theory and slender-body theory. *Biophys. J.* 25:113
- Kaiser GE, Doetsch RN. 1975. Enhanced translational motion of *Leptospira* in viscous environments. *Nature* 255:656–657
- Kanehl P, Ishikawa T. 2014. Fluid mechanics of swimming bacteria with multiple flagella. *Phys. Rev. E* 89:042704
- Kasyap TV, Koch DL, Wu M. 2014. Hydrodynamic tracer

- diffusion in suspensions of swimming bacteria. *Phys. Fluids* 26:081901
- Kaya T, Koser H. 2009. Characterization of hydrodynamic surface interactions of *Escherichia coli* cell bodies in shear flow. *Phys. Rev. Lett.* 103:138103
- Kaya T, Koser H. 2012. Direct upstream motility in *Escherichia coli*. *Biophys. J.* 102:1514–1523
- Kearns DB. 2010. A field guide to bacterial swarming motility. *Nature Rev. Microbiol.* 8:634–644
- Keller JB. 1974. Effect of viscosity on swimming velocity of bacteria. *Proc. Natl. Acad. Sci. USA* 71:3253–3254
- Keller JB, Rubinow SI. 1976. Swimming of flagellated microorganisms. *Biophys. J.* 16:151–170
- Kim M, Bird JC, Parys AJV, Breuer KS, Powers TR. 2003. A macroscopic scale model of bacterial flagellar bundling. *Proc. Natl. Acad. Sci. USA* 100:15481–15485
- Kim M, Powers TR. 2004. Hydrodynamic interactions between rotating helices. *Phys. Rev. E* 69:061910
- Kim MJ, Breuer KS. 2004. Enhanced diffusion due to motile bacteria. *Phys. Fluids* 16:L78–L81
- Kim MJ, Powers TR. 2005. Deformation of a helical filament by flow and electric or magnetic fields. *Phys. Rev. E* 71:021914–1–10
- Kim S, Karrila JS. 1991. *Microhydrodynamics: Principles and Selected Applications*. Boston, MA: Butterworth-Heinemann
- Koch DL, Subramanian G. 2011. Collective hydrodynamics of swimming microorganisms: Living fluids. *Annu. Rev. Fluid Mech.* 43:637 – 659
- Lauga E. 2007. Propulsion in a viscoelastic fluid. *Phys. Fluids* 19:083104
- Lauga E. 2014. Locomotion in complex fluids: Integral theorems. *Phys. Fluids* 26:081902
- Lauga E, DiLuzio WR, Whitesides GM, Stone HA. 2006. Swimming in circles: Motion of bacteria near solid boundaries. *Biophys. J.* 90:400–412
- Lauga E, Powers TR. 2009. The hydrodynamics of swimming microorganisms. *Rep. Prog. Phys.* 72:096601
- Leifson E. 1960. *Atlas of Bacterial Flagellation*. New York and London: Academic Press
- Lemelle L, Palierne JF, Chatre E, Vaillant C, Place C. 2013. Curvature reversal of the circular motion of swimming bacteria probes for slip at solid/liquid interfaces. *Soft Matter* 9:9759–9762
- Leshansky AM. 2009. Enhanced low-Reynolds-number propulsion in heterogeneous viscous environments. *Phys. Rev. E* 80:051911
- Li G, Tam LK, Tang JX. 2008. Amplified effect of brownian motion in bacterial near-surface swimming. *Proc. Natl. Acad. Sci. USA* 105:18355–18359
- Liao Q, Subramanian G, DeLisa MP, Koch DL, Wu MM. 2007. Pair velocity correlations among swimming *Escherichia coli* bacteria are determined by force-quadrupole hydrodynamic interactions. *Phys. Fluids* 19:061701
- Lighthill J. 1975. *Mathematical Biofluidynamics*. Philadelphia: SIAM
- Lighthill J. 1976. Flagellar hydrodynamics—The John von Neumann lecture, 1975. *SIAM Rev.* 18:161–230
- Lim S, Peskin CS. 2012. Fluid-mechanical interaction of flexible bacterial flagella by the immersed boundary method. *Phys. Rev. E* 85:036307
- Lin Z, Thiffeault JL, Childress S. 2011. Stirring by squirmers. *J. Fluid Mech.* 669:167–177
- Liu B, Breuer KS, Powers TR. 2013. Helical swimming in stokes flow using a novel boundary-element method. *Phys. Fluids* 25:061902
- Liu B, Breuer KS, Powers TR. 2014a. Propulsion by a helical flagellum in a capillary tube. *Phys. Fluids* 26:011701
- Liu B, Gulino M, Morse M, Tang JX, Powers TR, Breuer KS. 2014b. Helical motion of the cell body enhances caulobacter crescentus motility. *Proc. Natl. Acad. Sci. U.S.A.* 111:11252–11256
- Liu B, Powers TR, Breuer KS. 2011. Force-free swimming of a model helical flagellum in viscoelastic fluids. *Proc. Natl. Acad. Sci. USA* 108:19516–19520
- Lopez D, Lauga E. 2014. Dynamics of swimming bacteria at complex interfaces. *Phys. Fluids* 26:071902
- Lytle DA, Johnson CH, Rice EW. 2002. A systematic comparison of the electrokinetic properties of environmentally important microorganisms in water. *Colloid. Surf. B* 24:91–101
- Macnab RM. 1977. Bacterial flagella rotating in bundles: A study in helical geometry. *Proc. Natl. Acad. Sci. USA* 74:221
- Madigan MT, Martinko JM, Stahl D, Clark DP. 2010. *Brock Biology of Microorganisms (13th Edition)*. San Francisco, CA: Benjamin Cummings
- Magariyama Y, Ichiba M, Nakata K, Baba K, Ohtani T, et al. 2005. Difference in bacterial motion between forward and backward swimming caused by the wall effect. *Biophys. J.* 88:3648–3658
- Magariyama Y, Kudo S. 2002. A mathematical explanation of an increase in bacterial swimming speed with viscosity in linear-polymer solutions. *Biophys. J.* 83:733–739
- Magariyama Y, Sugiyama S, Kudo S. 2001. Bacterial swimming speed and rotation rate of bundled flagella. *Fems Microbiol. Lett.* 199:125–129
- Magariyama Y, Sugiyama S, Muramoto K, Kawagishi I, Imae Y, Kudo S. 1995. Simultaneous measurement of bacterial flagellar rotation rate and swimming speed. *Biophys. J.* 69:2154–2162
- Männik J, Driessen R, Galajda P, Keymer JE, Dekker C. 2009. Bacterial growth and motility in sub-micron constrictions. *Proc. Natl. Acad. Sci. USA* 106:14861–14866
- Marcos, Fu HC, Powers TR, Stocker R. 2012. Bacterial rheotaxis. *Proc. Natl. Acad. Sci. U.S.A.* 109:4780–4785
- Martinez VA, Schwarz-Linek J, Reufer M, Wilson LG, Morozov AN, Poon WCK. 2014. Flagellated bacterial motility in polymer solutions. *Proc. Natl. Acad. Sci. U.S.A.* 111:17771–17776
- Miño GL, Dunstan J, Rousselet A, Clément E, Soto R. 2013. Induced diffusion of tracers in a bacterial suspension: Theory and experiments. *J. Fluid Mech.* 729:423–444
- Mitchell JG. 2002. The energetics and scaling of search strategies in bacteria. *Am. Natur.* 160:727–740
- Morse M, Huang A, Li G, Maxey MR, Tang JX. 2013. Molecular adsorption steers bacterial swimming at the air/water interface. *Biophys. J.* 105:21 – 28
- Namba K, Vonderviszt F. 1997. Molecular architecture of bacterial flagellum. *Q. Rev. Biophys.* 30:1–65
- Olson SD, Lim S, Cortez R. 2013. Modeling the dynamics of an elastic rod with intrinsic curvature and twist using a regularized Stokes formulation. *J. Comp. Phys.* 238:169–187
- Ottemann KM, Miller JF. 1997. Roles for motility in bacterial-host interactions. *Mol. Microbiol.* 24:1109–1117
- Pedley TJ, Kessler JO. 1992. Hydrodynamic phenomena in suspensions of swimming microorganisms. *Annu. Rev.*

- Fluid Mech.* 24:313–358
- Phan-Thien N, Tran-Cong T, Ramia M. 1987. A boundary-element analysis of flagellar propulsion. *J. Fluid Mech.* 184:533–549
- Purcell EM. 1977. Life at low Reynolds number. *Am. J. Phys.* 45:3–11
- Purcell EM. 1997. The efficiency of propulsion by a rotating flagellum. *Proc. Natl. Acad. Sci. USA* 94:11307–11311
- Pushkin DO, Shum H, Yeomans JM. 2013. Fluid transport by individual microswimmers. *J. Fluid Mech.* 726:5–25
- Qian B, Jiang H, Gagnon DA, Breuer KS, Powers TR. 2009. Minimal model for synchronization induced by hydrodynamic interactions. *Phys. Rev. E* 80:061919
- Ramia M, Tullock DL, Phan-Thien N. 1993. The role of hydrodynamic interaction in the locomotion of microorganisms. *Biophys. J.* 65:755–778
- Reichert M, Stark H. 2005. Synchronization of rotating helices by hydrodynamic interactions. *Eur. Phys. J. E* 17:493–500
- Reid SW, Leake MC, Chandler JH, Lo CJ, Armitage JP, Berry RM. 2006. The maximum number of torque-generating units in the flagellar motor of *Escherichia coli* is at least 11. *Proc. Natl. Acad. Sci. USA* 103:8066–8071
- Reigh SY, Winkler RG, Gompfer G. 2012. Synchronization and bundling of anchored bacterial flagella. *Soft Matt.* 8:4363–4372
- Rusconi R, Guasto JS, Stocker R. 2014. Bacterial transport suppressed by fluid shear. *Nature Phys.* 10:212–217
- Saintillan D. 2010a. Extensional rheology of active suspensions. *Phys. Rev. E* 81:056307
- Saintillan D. 2010b. The dilute rheology of swimming suspensions: A simple kinetic model. *J. Exp. Mech.* 50:1275
- Schneider W, Doetsch RN. 1974. Effect of viscosity on bacterial motility. *J. Bacteriol.* 117:696–701
- Schnitzer MJ. 1993. Theory of continuum random walks and application to chemotaxis. *Phys. Rev. E* 48:2553
- Shaevitz JW, Lee JY, Fletcher DA. 2005. *Spiroplasma* swim by a processive change in body helicity. *Cell* 122:941
- Shoesmith JG. 1960. The measurement of bacterial motility. *J. Gen. Microbiol.* 22:528–535
- Silverman M, Simon M. 1974. Flagellar rotation and the mechanism of bacterial motility. *Nature* 249:73–74
- Sokolov A, Apodaca MM, Grzybowski BA, Aranson IS. 2010. Swimming bacteria power microscopic gears. *Proc. Natl. Acad. Sci. USA* 107:969–974
- Sokolov A, Aranson IS. 2009. Reduction of viscosity in suspension of swimming bacteria. *Phys. Rev. Lett.* 103:148101
- Son K, Guasto JS, Stocker R. 2013. Bacteria can exploit a flagellar buckling instability to change direction. *Nature Phys.* 9:494–498
- Spagnolie SE, ed. 2015. *Complex Fluids in Biological Systems*. Biological and Medical Physics, Biomedical Engineering. Springer, New York
- Spagnolie SE, Lauga E. 2011. Comparative hydrodynamics of bacterial polymorphism. *Phys. Rev. Lett.* 106:058103
- Spagnolie SE, Lauga E. 2012. Hydrodynamics of self-propulsion near a boundary: predictions and accuracy of far-field approximations. *J. Fluid Mech.* 700:105–147
- Spagnolie SE, Liu B, Powers TR. 2013. Locomotion of helical bodies in viscoelastic fluids: Enhanced swimming at large helical amplitudes. *Phys. Rev. Lett.* 111:068101
- Srigiriraju SV, Powers TR. 2006. Model for polymorphic transitions in bacterial flagella. *Phys. Rev. E* 73:011902
- Stocker R, Seymour JR. 2012. Ecology and physics of bacterial chemotaxis in the ocean. *Microbiol. Mol. Biol. Rev.* 76:792–812
- Taylor GI. 1967. Low Reynolds number flows. *US Natl. Comm. Fluid Mech. Films video*
- Turner L, Ryu WS, Berg HC. 2000. Real-time imaging of fluorescent flagellar filaments. *J. Bacteriol.* 182:2793–2801
- Vanloosdrecht MCM, Lyklema J, Norde W, Zehnder AJB. 1990. Influence of interfaces on microbial activity. *Microbiol. Rev.* 54:75–87
- Vig DK, Wolgemuth CW. 2012. Swimming dynamics of the Lyme disease spirochete. *Phys. Rev. Lett.* 109:218104
- Vigeant MAS, Ford RM. 1997. Interactions between motile *Escherichia coli* and glass in media with various ionic strengths, as observed with a three-dimensional tracking microscope. *Appl. Environ. Microbiol.* 63:3474–3479
- Vogel R, Stark H. 2010. Force-extension curves of bacterial flagella. *Eur. Phys. J. E* 33:259–271
- Vogel R, Stark H. 2012. Motor-driven bacterial flagella and buckling instabilities. *Eur. Phys. J. E* 35:1–15
- Vogel R, Stark H. 2013. Rotation-induced polymorphic transitions in bacterial flagella. *Phys. Rev. Lett.* 110:158104
- Vogel S. 1996. *Life in Moving Fluids*. Princeton, NJ: Princeton University Press
- Wada H, Netz RR. 2007. Model for self-propulsive helical filaments: Kink-pair propagation. *Phys. Rev. Lett.* 99:108102
- Wada H, Netz RR. 2008. Discrete elastic model for stretching-induced flagellar polymorphs. *EPL* 82
- Watari N, Larson RG. 2010. The hydrodynamics of a run-and-tumble bacterium propelled by polymorphic helical flagella. *Biophys. J.* 98:12–17
- Weibull C. 1950. Electrophoretic and titrimetric measurements on bacterial flagella. *Acta. Chim. Scandinav.* 4:260–267
- Wilking JN, Angelini TE, Seminara A, Brenner MP, Weitz DA. 2011. Biofilms as complex fluids. *MRS Bull.* 36:385–391
- Wolfe AJ, Conley MP, Berg HC. 1988. Acetyladenylate plays a role in controlling the direction of flagellar rotation. *Proc. Natl. Acad. Sci. U.S.A.* 85:6711–6715
- Wu XL, Libchaber A. 2000. Particle diffusion in a quasi-two-dimensional bacterial bath. *Phys. Rev. Lett.* 84:3017–3020
- Xie L, Altindal T, Chattopadhyay S, Wu XL. 2011. Bacterial flagellum as a propeller and as a rudder for efficient chemotaxis. *Proc. Natl. Acad. Sci. USA* 108:2246–2251
- Yuan J, Fahrner KA, Turner L, Berg HC. 2010. Asymmetry in the clockwise and counterclockwise rotation of the bacterial flagellar motor. *Proc. Natl. Acad. Sci. U.S.A.* 107:12846–12849
- Zhang L, Peyer KE, Nelson BJ. 2010. Artificial bacterial flagella for micromanipulation. *Lab Chip* 10:2203–2215
- Zhou S, Sokolov S, Lavrentovich OD, Aranson IS. 2014. Living liquid crystals. *Proc. Natl. Acad. Sci. U.S.A.* 111:1265–1270